Stochastic electron gas theory of coherence in laser-driven synchrotron radiation

F. V. Hartemann
Institute for Laser Science and Applications, Lawrence Livermore National Laboratory, Livermore, California 94550

(Received 1 July 1999; revised manuscript received 15 September 1999)

The transition from coherent to incoherent laser-driven synchrotron radiation is studied within the framework of a stochastic electron gas model. The fundamental difference between this approach and a relativistic fluid model resides in the fact that, for any number of incoherently phased point electrons, the 4-current contains Fourier components at arbitrarily short wavelengths, whereas the fluid model introduces an unphysical cutoff scale.

PACS number(s): 41.60.−m, 42.50.Ar, 41.75.Ht, 52.40.Nk

The main thrust of this Brief Report is the detailed study of the radiation characteristics of a relativistic electron distribution interacting with a laser pulse of arbitrary intensity, with a special emphasis on the coherence [1–4] properties of the scattered light. This work is motivated in part by recent experimental results, where high-intensity lasers using chirped pulse amplification (CPA) [5–7] have been used to pump free electrons to produce harmonics [8], and to drive relativistic electron beams to generate short-wavelength radiation, as exemplified by the E-144 experiment at SLAC [9]; this work is also stimulated by the growing interest in the development of laser-based advanced light sources, including the γ-γ collider and free-electron lasers (FEL's) operating in the self-amplified spontaneous-emission mode [10].

The transition from coherent to incoherent laser-driven synchrotron radiation is studied within the framework of a stochastic electron gas (SEG) model, where the statistical distribution of the initial electron phase is explicitly taken into account. In contrast with the simplistic linear scaling of the intensity with the number of electrons, an expression describing the degree of coherence of the radiation is derived, which depends on the ratio of the bunch to the radiation wavelength.

We first review the motion of an electron in the external laser field [11–13]: the length scale of the problem is c/ω_0, while time can be measured in units of $1/\omega_0$, charge in units of e, and mass in units of m_0. The electron motion is driven by the Lorentz force $du_\mu/d\tau=-F_{\mu\nu}u^\nu$, where $u_\mu(\tau)=dx_\mu/d\tau=\gamma(1,\beta)$ is the 4-velocity and τ is the proper time along the electron world line $x_\mu(\tau)$. The field tensor is defined in terms of the 4-potential as $F_{\mu\nu}=\partial_\mu A_\nu-\partial_\nu A_\mu$; for our purpose, a plane-wave model is sufficient: the 4-potential is given by $A_\mu(x_\nu)=[0,\mathbf{A}_\perp(\phi),0]$, where $\phi=k_\mu x^\mu(\tau)=t-z$, and satisfies the Lorentz gauge condition, $\partial_\mu A^\mu=0$. The electromagnetic field is

$$\mathbf{E}=\mathbf{E}_\perp=-\partial_t\mathbf{A}_\perp=-\frac{\partial\phi}{\partial t}\frac{d\mathbf{A}_\perp}{d\phi}=-\frac{d\mathbf{A}_\perp}{d\phi} \tag{1}$$

and

$$\mathbf{B}=\mathbf{B}_\perp=\nabla\times\mathbf{A}_\perp=\hat{z}\partial_z\times\mathbf{A}_\perp=\hat{z}\times\frac{\partial\phi}{\partial z}\frac{d\mathbf{A}_\perp}{d\phi}=-\hat{z}\times\frac{d\mathbf{A}_\perp}{d\phi}. \tag{2}$$

As $\mathbf{u}\times\hat{z}\times d\mathbf{A}_\perp/d\phi=[\mathbf{u}_\perp\cdot(d\mathbf{A}_\perp/d\phi)]\hat{z}-u_z(d\mathbf{A}_\perp/d\phi)$, the force equation can be separated into a transverse and an axial component: $d\mathbf{u}_\perp/d\tau=(\gamma-u_z)d\mathbf{A}_\perp/d\phi$ and $du_z/d\tau=\mathbf{u}_\perp\cdot(d\mathbf{A}_\perp/d\phi)=d\gamma/d\tau$. Using the light-cone variable, $\kappa=d\phi/d\tau=\gamma-u_z$, we recover the transverse momentum invariant, $\mathbf{u}_\perp-\mathbf{A}_\perp$; κ itself is invariant: $\kappa=\kappa_0=\gamma_0(1-\beta_0)$. The dynamics of a single electron within the laser field are now completely defined:

$$\mathbf{u}_\perp(\tau)=\mathbf{A}_\perp(\phi),\quad u_z(\tau)=u_0+(\kappa_0^{-1}/2)\,\mathbf{A}_\perp^2(\phi),$$
$$\text{and}\quad \gamma_z(\tau)=\gamma_0+(\kappa_0^{-1}/2)\,\mathbf{A}_\perp^2(\phi). \tag{3}$$
$$x_\mu(\phi)=x_\mu(\phi=0)+\int_0^\phi(dx_\mu/d\tau)(d\tau/d\psi)d\psi$$
$$=x_{\mu0}+\kappa_0^{-1}\int_0^\phi u_\mu(\psi)d\psi$$

is the electron 4-position; for a number of independent electrons, provided that space-charge effects can be neglected, the dynamics are identical, except for the fact that the initial positions vary.

Using ϕ as the independent variable, the distribution of photons radiated per unit solid angle per unit frequency is [14]

$$\frac{d^2N_\gamma(\omega,\hat{n})}{d\omega\,d\Omega}=\frac{a}{4\pi^2}\frac{\omega}{\kappa_0^2}\left|\sum_{n=1}^{N_e}\int_{-\infty}^{+\infty}\hat{n}\times[\hat{n}\times\mathbf{u}_n(\phi)]\times\exp\{i\omega[\phi+z_n(\phi)-\hat{n}\cdot\mathbf{x}_n(\phi)]\}d\phi\right|^2, \tag{4}$$

where N_γ is the photon number, $\hat{n}$ is the unit vector in the direction of observation, a is the fine-structure constant, and N_e is the electron number; as discussed above, $\mathbf{u}_n(\phi)$ can be replaced by the single-electron result obtained in Eq. (3).

For backscattered radiation,

$$\frac{d^2N_\gamma(\omega,\hat{z})}{d\omega\,d\Omega}=\frac{a}{4\pi^2}\frac{\omega}{\kappa_0^2}\left|\sum_{n=1}^{N_e}\int_{-\infty}^{+\infty}\mathbf{A}_\perp(\phi)\times\exp\{i\omega[\phi+2z_n(\phi)]\}d\phi\right|^2;$$

the axial position of each radiating electron must be specified:

$$z_n(\phi)=z_n+\frac{u_0}{\kappa_0}\phi+\frac{1}{2\kappa_0^2}\int_0^{\phi}\mathbf{A}_\perp^2(\psi)d\psi, \tag{5}$$

where z_n is the initial position of the nth electron. $\int_0^\phi \mathbf{A}_\perp^2(\psi)d\psi$ represents the relativistic mass correction of the ''dressed'' electron within the high-intensity laser pulse. The integral over phase and the sum over electrons separate:

$$\frac{d^2N_\gamma(\omega,-\hat{z})}{d\omega\, d\Omega}=\frac{a}{4\pi^2}\chi\left|\int_{-\infty}^{+\infty}\mathbf{A}_\perp(\phi)\right.$$
$$\left.\times\exp\left\{i\chi\left[\phi+\int_0^\phi \mathbf{A}_\perp^2(\psi)d\psi\right]\right\}d\phi\right|^2$$
$$\times\left|\sum_{n=1}^{N_e}\exp(i2\omega z_n)\right|^2. \tag{6}$$

Here, $\chi=\omega[(1+\beta_0)/(1-\beta_0)]$ is the normalized Doppler-shifted frequency, and $|\Sigma_{n=1}^{N_e}\exp(i2\omega z_n)|^2$ is the coherence factor [10].

In the case of a uniform initial electron distribution with random phase, illustrated in Fig. 1 (top), the coherence factor is simply the amplitude of a sum of phasors, each with unit length and a random angle θ. To show that the average length of the sum is given by $\sqrt{N_e}$, we use a proof by recurrence: first assume that the average length of the first n phasors is $\sqrt{n}$; we now add a vector of unit length with random orientation, as shown in Fig. 1 (middle), and the new vector has a length given by $\sqrt{(\sqrt{n}+\cos\theta)^2+\sin^2\theta}=\sqrt{n+1+2\sqrt{n}\cos\theta}$. To obtain the new average length, we integrate over θ:

$$\langle\sqrt{|(\sqrt{n}+\cos\theta)\hat{x}+\hat{y}\sin\theta|^2}\rangle=\left[n+1+\frac{\sqrt{n}}{\pi}\int_0^{2\pi}\cos\theta\, d\theta\right]^{1/2}$$
$$=\sqrt{n+1}, \tag{7}$$

which proves the recurrence.

We have thus shown that $\langle|\Sigma_{n=1}^{N_e}\exp(i\theta_n)|^2\rangle=N_e$; this result is independent of the radiation frequency, because there are no boundary conditions defining a length scale. In a realistic situation, the initial electron distribution defines a transition from coherent to incoherent radiation for a given wavelength. To properly model this situation, the derivation presented above must be modified: the key point is to replace the average over θ by a weighted average including the probability density of the initial phase. As derived previously, the length $L(n+1)$ of $n+1$ phasors is

$$L^2(n+1)=[L(n)+\cos\theta]^2+\sin^2\theta$$
$$=L^2(n)+1+2L(n)\cos\theta; \tag{8}$$

averaging over θ, and taking the limit where $n\gg 1$, we find that

$$L(n)\simeq\sqrt{n(1-\langle\cos\theta\rangle^2)}+n\langle\cos\theta\rangle, \tag{9}$$

with a relative error equal to $1/\sqrt{n}$. The accuracy of this solution is illustrated in Fig. 2 (top), where the behavior of

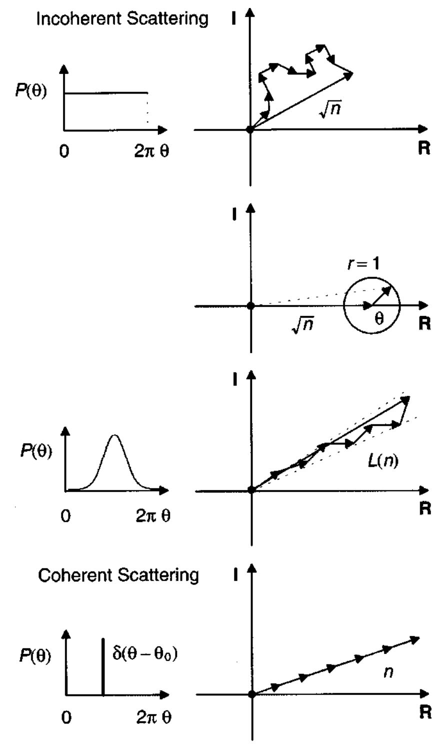

FIG. 1. Phasor summation and phase angle probability density for (from top to bottom) incoherent, partially coherent, and fully coherent scattering.

$L(n)$, calculated exactly with a computer, is shown as a function of $\langle\cos\theta\rangle$, and compared to Eq. (9) for $n=10^6$; the precision is excellent. The averaging over the random phase angle must now be specified:

$$\langle\cos\theta\rangle=\int_{-\infty}^{+\infty}P(\theta)\cos[\theta(z)]d\theta, \tag{10}$$

where $P(\theta)$ is the probability density for the initial phase of the electron. $P(\theta)$ is directly related to the initial electron distribution by the relation $\theta=2\omega z$, and is normalized: $\int_{-\infty}^{+\infty}P(\theta)d\theta=1$. Here, a Gaussian bunch of width Δz is considered; the probability density takes the form $P[\theta(z)]=(1/\sqrt{\pi}2\omega\Delta z)\exp[-(z/\Delta z)^2]$, and the average over θ is

$$\langle\cos\theta\rangle=\eta(a)=\sqrt{\frac{a}{\pi}}\int_{-\infty}^{+\infty}e^{-a\theta^2}\cos\theta\, d\theta, \tag{11}$$

where $a=(1/2\omega\Delta z)^2$. This integral yields $\langle\cos\theta\rangle=\exp(-\omega^2\Delta z^2)=e^{-1/2a}$.

If the electron distribution is much longer than $\lambda=2\pi c/\omega$, $\langle\cos\theta\rangle=0$, and the radiation is incoherent. When the electron distribution is much shorter than λ, the probability density distribution approaches a Dirac δ function, with $\lim_{a\to\infty}[\sqrt{(a/\pi)}e^{-a\theta^2}]=\delta(\theta)$, and the radiated power scales as N_e^2. This is illustrated in Fig. 1: for incoherent scattering (top), each phasor angle has equal probability; $\langle\cos\theta\rangle=0$, and the resulting superposition increases as $\sqrt{n}$. The case of fully coherent radiation is shown in Fig. 1 (bottom); here the angular probability density is a Dirac δ function, where $P(\theta)=\delta(\theta-\theta_0)$; the interference term $\langle\cos\theta\rangle=1$, and the phasor sum increases as n. Finally, an intermediate case is shown in Fig. 1 (middle); here the probability density indi-

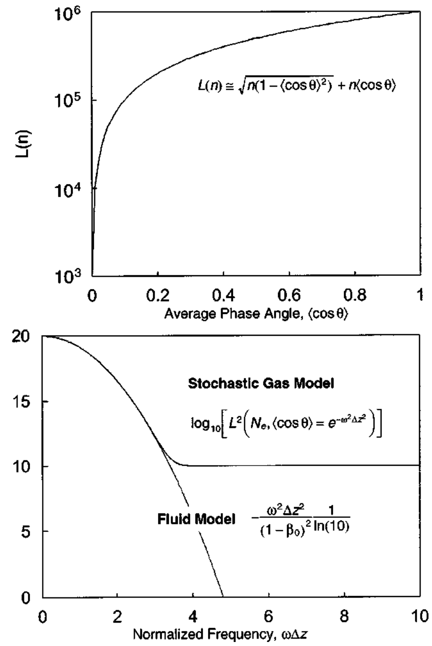

FIG. 2. Top: comparison between the average length of $n = 10^6$ phasors, as calculated exactly with a computer, and as derived from Eq. (9). Bottom: logarithm of the effective number of radiating electrons as a function of the normalized bunch length, for both models.

cates a preferred angular range, resulting in a superposition with an average length increasing as shown in Eq. (9).

Thus, the power backscattered by an electron bunch is given by

$$\frac{d^2N_\gamma(\omega,-\hat{z})}{d\omega\, d\Omega} = \frac{a\chi}{4\pi^2}L^2(N_e, e^{-\omega^2\Delta z^2})\left|\int_{-\infty}^{+\infty}\mathbf{A}_\perp(\phi)\times\exp\left\{i\chi\left[\phi+\int_0^\phi \mathbf{A}_\perp^2(\psi)d\psi\right]\right\}d\phi\right|^2. \quad (12)$$

and depends explicitly on the wavelength and bunch size. For a linearly polarized Gaussian pulse, where $\mathbf{A}_\perp(\phi) = A_0\hat{x}e^{-i\phi-(\phi/\Delta\phi)^2}$, and with $A_0^2 \ll 1$, the Fourier transform yields

$$\frac{d^2N_\gamma(\omega,-\hat{z})}{d\omega\, d\Omega} = \frac{a}{16\pi}\chi A_0^2\Delta\phi^2 L^2(N_e, e^{-\omega^2\Delta z^2})\times\exp\left[-\frac{(\chi-1)^2\Delta\phi^2}{2}\right]. \quad (13)$$

In the case of circular polarization, for a hyperbolic secant pulse, the full nonlinear spectrum can be determined analytically [13]:

$$\frac{d^2N_\gamma(\omega,-\hat{z})}{d\omega\, d\Omega} = \frac{a}{8}\chi A_0^2\Delta\phi^2 L^2(N_e, e^{-\omega^2\Delta z^2})\times\left\{\sum_\pm\left|\frac{\Phi(\mu_\pm, 1, 2iA_0^2\chi\Delta\phi)}{\cosh\left[\frac{\pi}{2}\Delta\phi(\chi\pm 1)\right]}\right|^2\right\}, \quad (14)$$

where Φ is the degenerate hypergeometric function and $\mu_\pm = \frac{1}{2}[1+i\Delta\phi(\chi\pm1)]$. The frequency downshift due to radiation pressure is determined by considering the nonlinear phase, $\Lambda(\phi) = (\chi-1)\phi + \chi A_0^2\Delta\phi\tanh(\phi/\Delta\phi)$, in the Fourier integral; Taylor expanding around $\phi=0$, we obtain $\Lambda(\phi) \simeq [\chi(1+A_0^2)-1]\phi + O(\phi^3)$. The frequency of the Compton backscattered line is obtained by canceling the linear coefficient, yielding $\chi = (1+A_0^2)^{-1}$; this is the well-known radiation frequency for a FEL with an electromagnetic wiggler [15].

To compare the SEG to a relativistic fluid, we now consider the Lorentz force equation $du_\mu/d\tau = (u^\nu\partial_\nu)u_\mu = -(\partial_\mu A_\nu - \partial_\nu A_\mu)u^\nu$ and the charge-conservation equation $\partial_\mu j^\mu = 0$. Here, $u_\mu(x_\nu)$ is the 4-velocity field of the relativistic fluid, and $d/d\tau$ is to be considered as a convective operator. The 4-current density of the relativistic fluid is given by $j_\mu(x_\nu) = -n(x_\nu)[u_\mu(x_\nu)/\gamma(x_\nu)]$, where $n(x_\nu)$ is the density. Space-charge and radiation reaction [13,16,17] effects are neglected.

As the force equation is driven by the laser 4-potential, which is a function of the fluid phase, $\phi(z,t) = t - z$, we seek a solution where the other fluid fields also depend on ϕ: the convective derivative operator reduces to $(u^\nu\partial_\nu)u_\mu(z,t) \equiv (\gamma - u_z)du_\mu/d\phi$. The Lorentz force equation now reads $(\gamma-u_z)d\mathbf{u}/d\phi = -(\gamma\mathbf{E}+\mathbf{u}\times\mathbf{B})$; in addition, energy conservation yields $(\gamma-u_z)d\gamma/d\phi = -\mathbf{u}\cdot\mathbf{E}$. The fields are given in Eqs. (1) and (2).

The evolution of the momentum field is separated into a transverse and an axial component: $(\gamma-u_z)d/d\phi(\mathbf{u}_\perp - \mathbf{A}_\perp) = \mathbf{0}$ and $(\gamma-u_z)du_z/d\phi = \mathbf{u}_\perp\cdot(d\mathbf{A}_\perp/d\phi) = (\gamma-u_z)d\gamma/d\phi$. We recover the transverse momentum invariant, $\mathbf{u}_\perp - \mathbf{A}_\perp$; the light-cone variable is also a fluid invariant. The sought-after fluid equilibrium is

$$u_z(z,t) = u_z(\phi) = u_{z0} + \kappa_0^{-1}\left[\mathbf{A}_\perp(\phi)\cdot\mathbf{u}_{\perp 0} + \frac{\mathbf{A}_\perp^2(\phi)}{2}\right], \quad (15)$$

and

$$\gamma(z,t) = \gamma(\phi) = \gamma_0 + \kappa_0^{-1}\left[\mathbf{A}_\perp(\phi)\cdot\mathbf{u}_{\perp 0} + \frac{\mathbf{A}_\perp^2(\phi)}{2}\right]. \quad (16)$$

To determine the density, we seek a solution to the charge-conservation equation where the density field is a function of the phase:

$$\frac{d}{d\phi}\left[\frac{n}{\gamma}(\gamma-u_z)\right] = \frac{d}{d\phi}\left(\frac{n}{\gamma}\kappa\right) = \kappa_0\frac{d}{d\phi}\left(\frac{n}{\gamma}\right) = 0; \quad (17)$$

thus, the relativistic plasma frequency is a relativistic fluid invariant: $n(\phi)/\gamma(\phi) = n_0/\gamma_0$; the density modulation induced by the laser radiation pressure exactly compensates the variation of the fluid energy within the pulse. Here, n_0 is the initial beam density.

The distribution of energy radiated by the fluid per unit solid angle per unit frequency is derived by Fourier-transforming the 4-current into momentum space [14]:

$$\frac{d^2N_\gamma(\omega,\hat{n})}{d\omega\, d\Omega} = \frac{a}{4\pi^2}\omega\left|\int\int\int\int_{\mathbb{R}^4} d^4x_\mu \hat{n}\times[\hat{n}\times\mathbf{j}(x_\mu)]\exp[i\omega(t-\hat{n}\cdot\mathbf{x})]\right|^2. \quad (18)$$

where $\mathbf{j}(x_\mu)$ is given by $\mathbf{j}=-n\beta=-n_0(\gamma/\gamma_0)\beta=-(n_0/\gamma_0)\mathbf{u}$.

The initial beam density is $n_0(x_\mu)=\rho f(\zeta)$, where we have defined the electron-beam phase $\zeta(z,t)=z-\beta_0 t$, and where $f(\zeta)$ is the bunch envelope, which propagates with the axial velocity β_0; ρ is defined by the total charge in the bunch: $\rho\int_{-\infty}^{\infty}dz\, f(\zeta)=N_e$. This initial density field conserves charge. This model for the background fluid density is valid as long as its spatial and temporal gradients are small compared to k_0 and ω_0. We use a Gaussian profile to obtain an analytical result for the radiated spectra: $f(\zeta)=\exp[-(\zeta/\Delta z)^2]$ and $\rho=N_e/\sqrt{\pi}\Delta z$. Here, Δz is the bunch length, and a linearly polarized laser pulse, with temporal envelope $g(\phi)$, is considered:

$$\frac{d^2N_\gamma(\omega,-\hat{z})}{d\omega\, d\Omega}=\frac{a}{4\pi^2}\frac{\omega}{\gamma_0^2}\rho^2\mathbf{A}_0^2\left|\int\int_{\mathbb{R}^2}dz\, dt\, f(\zeta)g(\phi)\times\exp\{[\omega(t+z)-\phi]\}\right|^2. \quad (19)$$

The integrals over axial position and time are separated by using ζ and ϕ as independent variables. The product of the differential elements is given by the Jacobian

$$dz\, dt=\begin{vmatrix}\frac{\partial z}{\partial\phi} & \frac{\partial z}{\partial\zeta}\\ \frac{\partial t}{\partial\phi} & \frac{\partial t}{\partial\zeta}\end{vmatrix}d\phi\, d\zeta=\frac{-d\phi\, d\zeta}{1-\beta_0}, \quad (20)$$

and Eq. (19) reduces to

$$\frac{d^2N_\gamma(\omega,-\hat{z})}{d\omega\, d\Omega}=a\chi A_0^2\rho^2\left|\int_{-\infty}^{+\infty}d\zeta\exp\left[i\frac{2\chi\zeta}{1+\beta_0}-\frac{\zeta^2}{\Delta z^2}\right]\times\int_{-\infty}^{+\infty}d\phi\exp\left[i(\chi-1)\phi-\frac{\phi^2}{\Delta\phi^2}\right]\right|^2. \quad (21)$$

The first integral is the fluid coherence factor. Integrating over ϕ and ζ, we finally obtain

$$\frac{d^2N_\gamma(\omega,-\hat{z})}{d\omega\, d\Omega}=\frac{a}{16\pi}\chi A_0^2\Delta\phi^2N_e^2\exp\left[-2\left(\frac{\chi\Delta z}{1+\beta_0}\right)^2\right]\times\exp\left[-\frac{(\chi-1)^2\Delta\phi^2}{2}\right]. \quad (22)$$

The Compton backscattered frequency is obtained for $\chi=1$; for $\beta_0\to-1$, we recover the result $\omega\simeq4\gamma_0^2$ [13,15].

The SEG and relativistic fluid models are compared by inspecting Eqs. (13) and (22), in a frame where $\beta_0=0$. The difference between both models is shown in Fig. 2 (bottom), where the number of electrons is $N_e=10^{10}$. The logarithm of each coherence factor is calculated as a function of the normalized bunch length, $\omega\Delta z$. In the case of a perfectly coherent radiation process, $\omega\Delta z\to0$, and both models yield the N_e^2 scaling. When the electron distribution becomes long compared to the radiation wavelength, the SEG model correctly predicts the linear scaling with N_e. The fluid model yields a very different result: the coherence factor continues to decrease exponentially, as shown by the parabolic curve in Fig. 2 (bottom). This is due to the fact that the Fourier transform of the Gaussian fluid distribution is a Gaussian with an argument proportional to the product $\omega\Delta z$: for arbitrarily short wavelengths, the fluid 4-current yields a vanishingly small Fourier component. The fluid model introduces an unphysical cutoff scale given by the length of the electron distribution. Thus, the fundamental difference between the SEG approach and the relativistic fluid model resides in the fact that, for any number of incoherently phased point electrons, the 4-current contains Fourier components at arbitrarily short wavelengths, whereas the fluid model introduces an unphysical cutoff scale. Therefore, the discrete nature of electric charge is shown to play a fundamental role in the physics of incoherent radiation processes.

This work was partially supported by the Lawrence Livermore National Laboratory under DOE Contract No. W-7405-ENG-48. I would also like to thank C. Pellegrini. K. J. Kim, A. K. Kerman, J. Rosenzweig, J. R. Van Meter, and D. T. Santa Maria.

[1] R. J. Glauber, Phys. Rev. **130**, 2529 (1963).
[2] L. Mandel and E. Wolf, *Optical Coherence and Quantum Optics* (Cambridge University Press, Cambridge, 1995).
[3] R. Loudon, *The Quantum Theory of Light* (Oxford University Press, Oxford, 1983).
[4] R. H. Dicke, Phys. Rev. **93**, 99 (1954).
[5] M. D. Perry and G. Mourou, Science **264**, 917 (1994).
[6] G. A. Mourou, C. P. J. Barty, and M. D. Perry, Phys. Today **51** (1), 22 (1998).
[7] D. P. Umstadter, C. Barty, M. Perry, and G. A. Mourou, Opt. Photonics News **9**, 41 (1998).
[8] S. Y. Chen, A. Maksimchuk, and D. Umstadter, Nature (London) **396**, 653 (1998).
[9] C. Bamber, *et al.*. Phys. Rev. D **60**, 092004 (1999).
[10] M. Hogan *et al.*, Phys. Rev. Lett. **81**, 4867 (1998).
[11] L. S. Brown and T. W. B. Kibble, Phys. Rev. **133**, A705 (1964).
[12] E. S. Sarachik and G. T. Schappert, Phys. Rev. D **1**, 2738 (1970).
[13] F. V. Hartemann, Phys. Plasmas **5**, 2037 (1998).
[14] J. D. Jackson, *Classical Electrodynamics*, 2nd ed. (Wiley, New York, 1975).
[15] C. W. Roberson and P. Sprangle, Phys. Fluids B **1**, 3 (1989).
[16] P. A. M. Dirac, Proc. R. Soc. London, Ser. A **167**, 148 (1938).
[17] F. V. Hartemann and A. K. Kerman, Phys. Rev. Lett. **76**, 624 (1996).